

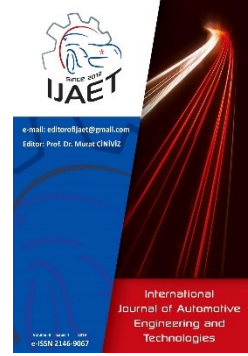


e-ISSN: 2146 - 9067

International Journal of Automotive Engineering and Technologies

journal homepage:

<https://dergipark.org.tr/en/pub/ijaet>



Original Research Article

Fuel-air mixing process of low pressure direct injection in a side ported rotary engine



Özgür Oğuz Taşkıran

Design Project Office, Turkish Naval Forces, Pendik, İstanbul, Turkey

ARTICLE INFO

ABSTRACT

* Corresponding author
taskiranoz@itu.edu.tr

Received: Aug 21, 2019
Accepted: Nov 21, 2019

Published by Editorial Board
Members of IJAET

© This article is distributed by
Turk Journal Park System under
the CC 4.0 terms and conditions.

Stratification is seen as a prominent technique for improving the performance of spark ignition engines especially at part loads. Though rotary engines have high specific power, they suffer high fuel consumption and HC emission. For this reason, direct injection methods in rotary engines have been investigated since they were introduced to the market. In this study, early direct injection in a side ported rotary engine was investigated by using CFD techniques. The aim of the study is to obtain the potential of low pressure direct injection method on mixture formation process. Geometrical model of Mazda Renesis engine that were modified as a single rotor engine for research activities was used in the modeling studies. Fuel was injected directly to the chamber from present oil hole location that has less geometrical constraints than any other location of the Renesis engine. Simulations were done for 2000 rpm which is a typical part load operation point of the engine. In numerical calculations, RNG k- ϵ model was used as the turbulence model; spray breakup was modeled by the Taylor Analogy Breakup (TAB) model. Flow pattern of intake air and fuel droplet distributions were investigated for a possibility of having rich mixture around spark plugs. The results showed that swirl-like motion of the side ported engine inhibits fuel spray to accumulate in the middle of the combustion chamber. Fuel droplets were driven to the counter side of the inlet wall by centrifugal force of the inlet air. This effect reduced as the swirl flow diminishes due to sweeping motion of the rotor. It is observed that the main flow in the chamber is converted to the tumble-like flow at middle and last part of the compression stroke.

Keywords: Rotary engine, direct injection, stratification, CFD engine modeling

1. Introduction

High power density of the Wankel type rotary engine (WTRE) is the key benefit among the other advantages such as simple design, having no cranking mechanism, less vibration and noise etc. The working principle of WTRE is based on four stroke cycle similar to reciprocating engine. The complete working cycle lasts 1080 ESA

(Eccentric Shaft Angle) in WTREs where it is 720 CA (Crankshaft Angle) in conventional reciprocating engines. WTREs carry three combustion chambers in single rotor giving three times higher power output for per rotation of the rotor.

The benefits of the WTRE attracted many companies and researchers. The studies showed that WTREs have some drawbacks compared to

the reciprocating engines such as high fuel consumption and high emission rates, due to leakage problems of sealing, short lifetime of the engine, narrow combustion chamber causing slow combustion etc. Hydrogen blended fuel usage for increasing combustion speed, gas seal improvements for leakage problems, port configuration change for increasing volumetric efficiency, direct injection stratified charge applications for improving fuel consumption were some potential improvements proposed to overcome these drawbacks. WTRE increased its popularity when Mazda RX series, rotary engine driven automobile, successfully demonstrated engine performance in vehicles. However, especially after 2000s, the commercial vehicles were subjected to strict emission restrictions. WTREs couldn't cope with reciprocating engines due to its high fuel consumption and emission problems; hence Mazda Company stopped using WTRE in their vehicles after 2012. The practical applications of the WTRE do not seem to have been increased then. They are preferred in power dense applications such as small portable machines, boats, light air vehicles etc. On the contrary, conventional reciprocating engines were undergone an evolution by the improvements on injection system, turbocharging system, EGR (Exhaust Gas Recirculation) application, control system, down-sizing, after treatment system and etc. Improvements on computer technology and new mathematical models have also considerable role on this evolution.

In order to defeat the drawbacks of WTRE, applicability of new methods and models are discussed in technical literature. The published studies on WTRE are divided in two main groups; the first one is experimental studies and the second one is theoretical mathematical models. Mathematical models of reciprocating engines are much more prevalent than rotary ones. Due to WTREs' eccentric motion, geometric model of the engine is not easily applicable to existing codes of reciprocating engines. However unusual geometrical shape brings some advantages in terms of port configuration. Inlet ports of the WTRE can be mounted both on periphery of the housing and side wall of the engine. It has been shown that performance of the engine can be improved by optimizing intake and exhaust by using side

ports [1-3].

The emphasis on the recent studies of WTRE is related to decreasing its fuel consumption to a level that is compatible with reciprocating engines. Especially at part loads, it is possible that if the fuel is injected directly to the combustion chamber rather than port injection, a stratified fuel air mixture can be obtained enabling more efficient engine. However, WTREs counter some limitations on direct injection strategies for a stratified charge. Though a late direct injection, near TDC is needed for a stratified charge, it is restricted by rotor movement because the edges of triangular shaped rotor sweep housing inner surface during their rotational movement. Furthermore, as the rotor moves to TDC, wide and long shape of the volume between rotor and housing does not allow spray to penetrate longer as it does in reciprocating engines. Successful implementation of a direct injection method can be achieved by making numerical investigation on injection location and its timing before making expensive experimental tests on WTREs. In literature, there are many studies focusing on direct injection methods to improve engine efficiency and emissions of peripheral ported rotary engine. However, the effect of side port configuration on these outputs was fairly investigated for direct injection methods. This study differs from the early studies as it investigates early direct injection method in respect to side ported configuration. The control of air flow and fuel spray plays a critical role on obtaining appropriate fuel distribution in the combustion chamber. Numerical analyses can improve direct injection implementing strategies such as injection timing or location. In this study, the potential of direct injection method by making an early injection at the beginning of compression stroke was reported.

2. Literature Review

The first appearance of WTRE in the automobile market was in 1967 with Mazda 110S. After then, a couple variant of 110S engine were produced. One of them is 10A engine, producing 100 hp at 7000 rpm, had cracking of the rotor housing and HC emission problems [4]. Later, 12A, 13A, 12B and 13B engines based on same structure of 10A were designed to produce higher power. Adopting

thermal reactors were the Mazda Co.'s principal approach to the control of CO and HC exhaust emissions in 1970s [5].

Another problem of the WTRE is leakage between seals. Low engine speed causes more leakage which reduces maximum torque, increases emissions and fuel consumption. Eberle et al [6] showed that engine performance can be improved by reducing leakage. Nguyen et al simulated direct injection stratified charge WTRE and they underlined that faster combustion, reduced leakage and turbocharging improve the performance of the rotary engines [7]. Jeng et al [8] showed that increased leakage may contribute to better mixing and combustion but reduces the indicated mean effective pressure. Model of Pickard et al [9] predicted that the side, apex and corner seals have approximately similar level of leakages.

Operating overall lean mixture, stratified charge engine studies based on two main approaches; direct injection in the vicinity of the plug and use of a pre-combustion chamber. Compared with carbureted WTRE, Jones [10] showed using both close coupled and dual injector reduced the fuel consumption considerably. In their proceeded works, Jones et al [11-13] also reported that HC, NO_x and CO emissions were reduced by using similar direct injection and stratified charge applications. Early injection was tested in Mazda 13B engine under the name of ROSCO and fuel reduction in low speed engine was obtained under the potential engine tests [14]. Another successful application of a direct injection stratified rotary engine for motor vehicles was made by Kagawa et al [15] with main injection into the chamber and pilot injection into the sub-chamber. Low pressure direct injection was studied by Hasegawa and Yamaguchi [16] with different rotor recess and they stated that stratification can be improved with putting recess to the leading side.

The rotor recess shape has importance in direct injection since it enables spray to penetrate into the chamber and direct it to the vicinity of spark plug. Moriyoshi et al [17] and Moruki et al [18] tested some rocket pocket geometries to study the fundamental process for direct injection. Their initial experiments were made on rapid compression machine not on a WTRE. Later, based on their prior experiments, Maroki et al

[19] applied a pilot flame ignition system on a WTRE and they obtained better fuel consumption at light loads than conventional WTRE. Study of Nai-jun et al [20] showed better combustion efficiency and lower NO emission obtained with middle located and shallower rotor recess.

The first three dimensional models of WTREs were done by Grasso et al [21] making a comprehensive analysis of flow field and combustion for homogenous charge and dual injection. Later, Abraham et al [22] showed non-uniform mixing of fuel and air leading long and incomplete combustion in stratified WTREs. Abraham and Bracco reported an analysis of direct injection rotary engine based on 3d numerical calculations, in which they focused on spray patterns [23] and ignition strategies [24].

Direct injection method also enables to use multi-fuels in WTREs. Jones [25] introduced Score engine which is a stratified charge WTRE having multi-fuel capability and diesel-level fuel economy. Mount and LaBouff et al [26] reported a successful application of advanced stratified rotary engine using multi-fuel. In a recent study, Lu et al reported the investigations on the use of aviation kerosene in rotary engines by means of different injection strategies [27]. Louthan [28] presented a conversion work of gasoline WTRE to JP-5 fuel for naval applications. This conversion resulted higher weighted and less powered engine. Boretta et al [29] proposed two jet ignition devices per rotor that are replacing the traditional two spark plugs of Renesis engine for a faster and more complete combustion. Recently, Fan et al [30] presented comparative simulations of three direct injection points during compression stroke period and obtained best result from the one close to the intake port.

The advances in fuel injection systems open new opportunities in WTREs. Meyer and Shoemaker [31] adopted common rail injection system to a WTRE and obtained almost similar performance with jerk pump system. Rake et al [32] presented Piezoelectric Controlled Carburetor (PCC) system for small engines, which decreases fuel consumption and emissions. The use of alternative fuels is also very promising in rotary engines. The hydrogen usage has many advantages such as decreasing

emissions, increasing combustion efficiency and higher power output [33]. The hydrogen injection strategy and nozzle injection diameter have influence on the flow behavior, flame propagation, combustion characteristics, and pollutants formation of rotary engines [34].

3. Methods and Numerical Model

Three possible direct injection points were demonstrated in Fig.1. The pros and cons of these injection points were discussed in [35]. Among them, Point-A having less pressure difference between chambers, low injection pressure necessity and locational advantages comes into prominence. In numerical point of view, spray injection from Point-B and C which have higher injection pressure than A may be modeled with different breakup models. For this reason, Point-A was chosen as injection point in this study. Injector was modeled with 4 nozzles each having 0.35 mm diameter.

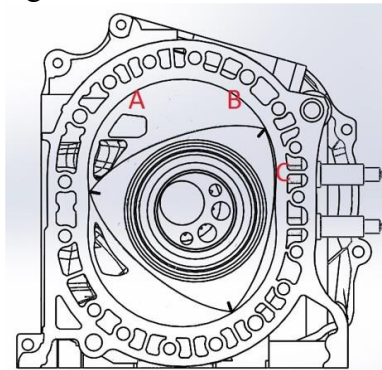


Figure 1. Proposed three injection points [32].

In numerical calculations, geometrical model of rotary engine that has 654 cc displacement and 10 compression ratio was used. Numerical model represents the experimental single rotor test engine that was constructed from a Mazda 13B-Renesis engine [36]. In order to obtain a realistic numerical model of the engine, all three chambers were included in the model as seen in Fig 2.

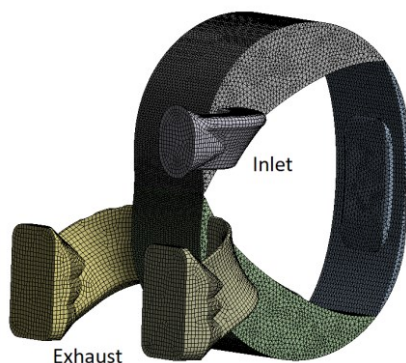


Figure 2. Numerical model of the single rotor WRE

Numerical model has 430000 cells containing tetrahedrons in combustion chamber and hex dominant cells in port channels. The eccentric motion of the rotor was simulated by using User Defined Function (UDF) of ANSYS-Fluent that enables dynamic mesh motion in the fluid region. Mesh dependency tests and validation of flow field were done on previous work [37]. Fuel was injected after one eccentric shaft revolution (360 ESA) for stabilization of initial and boundary conditions. Injected fuel mass is 28 mg for 4 bar mean effective pressure condition. It is aimed that the start of injection begins as late as possible to avoid inlet air disturbance. Air inlet and injection periods are shown in Fig. 3.

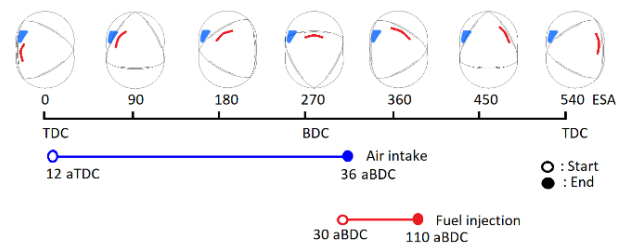


Figure 3. Air intake and fuel injection timing.

In Fluent, the fluid flow is solved by using the Navier-Stokes equations, while the discrete phase is solved by using Lagrangian formulation. Turbulence which has significant influence on in-cylinder flow simulations was modeled with $k-\epsilon$ based RNG model. In validation studies [37] it is shown that RNG model better represents flow structure. RNG model has effective viscosity term (μ_{eff}) and additional term (R_ϵ) given in the transport equation of ϵ improving the accuracy for rapidly strained flows;

$$R_\epsilon = \frac{C_\mu \rho \left(1 - \frac{S_k/\epsilon}{\eta_0}\right) \epsilon^2}{1 + \beta (S_k/\epsilon)^3} \frac{\epsilon^2}{k} \quad (1)$$

where C_μ is defined as 0.0845, S_k is user defined source term, and β is 0.012 [38].

Evaporation, collision and breakup models are important for a realistic spray model. In this study, droplet breakup was modeled by using Taylor Analogy Breakup (TAB) model, which is suitable for low pressure injection [38]. Breakup model has great importance since it governs droplet size distribution. For a damped and forced linear harmonic oscillator;

$$F - kx - d \frac{dx}{dt} = m \frac{d^2x}{dt^2} \quad (2)$$

where F is assumed as the external force that

comes from relative motion of droplet in fluid, x is the droplet equator displacement, k is restoring force of the droplet which equals to surface tension and d is the damping term equals to fluid dynamic viscosity. From this analogy;

$$\frac{F}{m} = C_F \frac{\rho_g u^2}{\rho_l r} \quad (3)$$

$$\frac{k}{m} = C_k \frac{\sigma}{\rho_l r^3} \quad (4)$$

$$\frac{d}{m} = C_d \frac{\mu_l}{\rho_l r^2} \quad (5)$$

the oscillation equation can be written as with non-dimensional parameter y ;

$$y = \frac{x}{C_b r} \quad (6)$$

and from the solution of y ;

$$\frac{d^2 y}{dt^2} = \frac{C_F \rho_g u^2}{C_b \rho_l r^2} - \frac{C_k \sigma}{\rho_l r^3} y - \frac{C_d \mu_l}{\rho_l r^2} \frac{dy}{dt} \quad (7)$$

obtained. Droplet breakup occurs where the distortion equals to droplet radius which means if y is greater than 1. The constants in the models, other sub-models, initial and boundary conditions are summarized in Table 1.

Table 1. Summary of sub-models, constants, initial and boundary conditions.

Subject	Input
Inlet/outlet temperatures	330/900 K
Rotor/housing wall temp.	473/423 K
Inlet/outlet pressure	0.06/0.1 MPa
Wall boundary	No-slip
Turbulence	RNG k- ϵ ($C_{1\epsilon}$:1.42, $C_{2\epsilon}$:1.68, β :0.012)
Press.-velocity coupling	PISO algorithm
Breakup model	TAB model (C_F : 1/3, C_k :8, C_d :5, C_b :0.5)
Droplet size distribution	Rosin-Rammler
Injected fuel mass	28 mg
Discretization scheme	Energy: 2nd or. upw. Momentum: 2nd or. upw. Density: 2nd or. upw. Turbulence: 1st or. upw.

4. Results and Discussion

Rotational movement of the rotor inside the housing restricts the available injection period for WTRE. The limits in reciprocating counterparts are different since they have stationary cylinder head. Time between the rotor leading and trailing edges passing over the injection point on housing is defined as maximum injection period. However, injection should not start as soon as leading edge passes

over the injection point in order to prevent wall wetting. The same is valid for the trailing side. For this reason, there should be appropriate time gap for droplet penetration without causing wall wetting. This time gap differs according to injection characteristics and engine geometry. As an average value, 120 ESA can be taken for spray injection retard. The plots in Fig. 4 show the maximum time period and applicable time period without wall wetting for simulated Point-A. The available period decreases below 8 ms after 5000 rpm. This short period restricts direct injection method to be applied at high load and rpm. In this study, it is accepted that injection direction is towards only to the leading edge. It should be noted that there will be no injection nozzle directed to the side walls or trailing side.

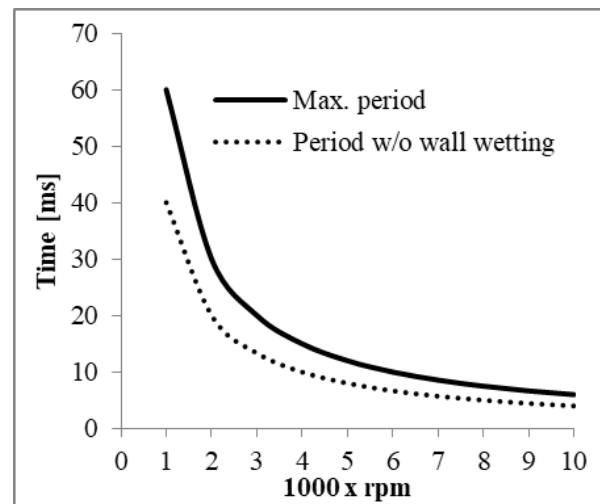


Figure 4. Maximum and available time period for injection at Point-A

The time resolved flow structure, spray penetration and fuel mass distribution were shown in Fig. 5-7 for mixture formation period. Fuel mass concentrations were shown on middle plane and rotor wall. In the middle of injection period, at 70 aBDC, the flow streamlines are seen in Fig. 5. The initial flow has swirl-like motion in the combustion chamber. It is seen that breakup occurs just after the spray droplets penetrates into the chamber. Small droplets are quickly driven by inlet air towards to the side wall and remaining larger droplets stay more close to the middle section of the chamber. However, as the chamber temperature increases during the compression stroke, droplets evaporate more quickly. As a result of breakup and evaporation, they get smaller and almost 90% percent of fuel droplets accumulate on the counter side of the inlet port (Fig. 5b).

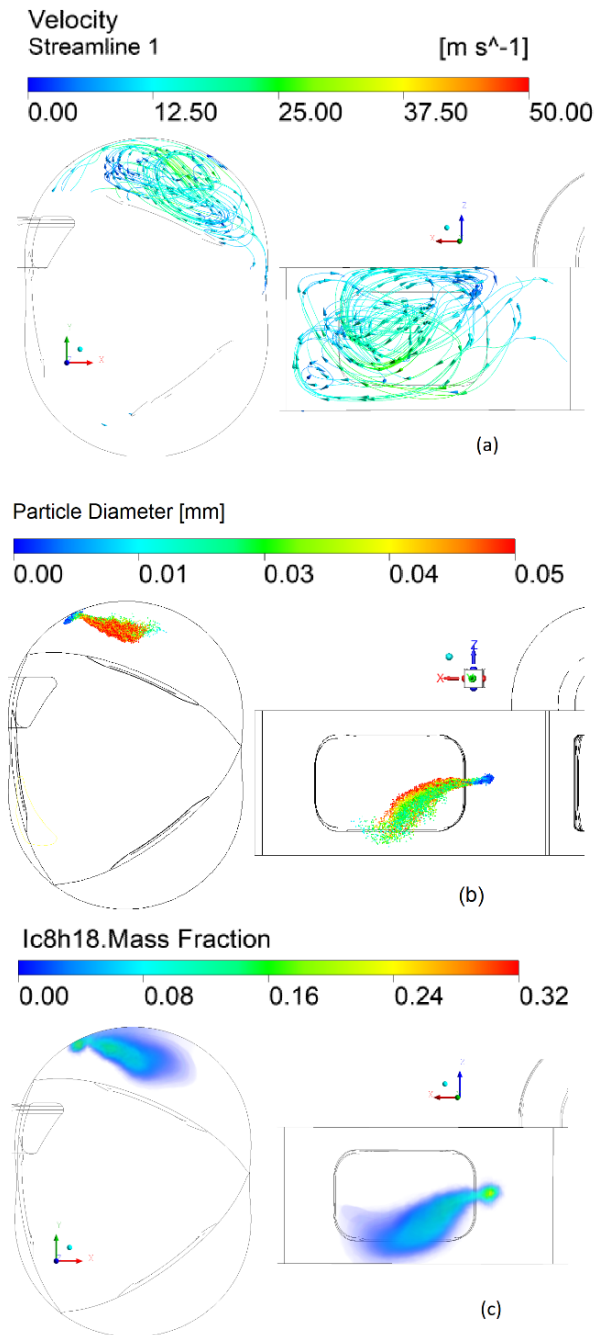


Figure 5. Mixture formation at the middle of injection period; (a) Flow velocity streamlines, (b) Droplet diameter and (c) Fuel mass fraction distributions at 70 ESA aBDC.

The flow inside the chamber evolves from swirl motion to tumble-like motion as the rotor proceeds in compression stroke. Since the mean flow velocity decreases to approximately 20 m/s, the flow motion decreases its effect on fuel mixture formation. It is shown in Fig. 6 that the evaporated droplets form fuel rich zone close to the side wall during the last part of the compression stroke. As a result, observed three factors at this stage, which are i) transient motion from swirl to tumble, ii) decrease of

velocity and iii) droplets accumulation on the counter side, do not allow generating fuel rich zone in the middle section of the chamber.

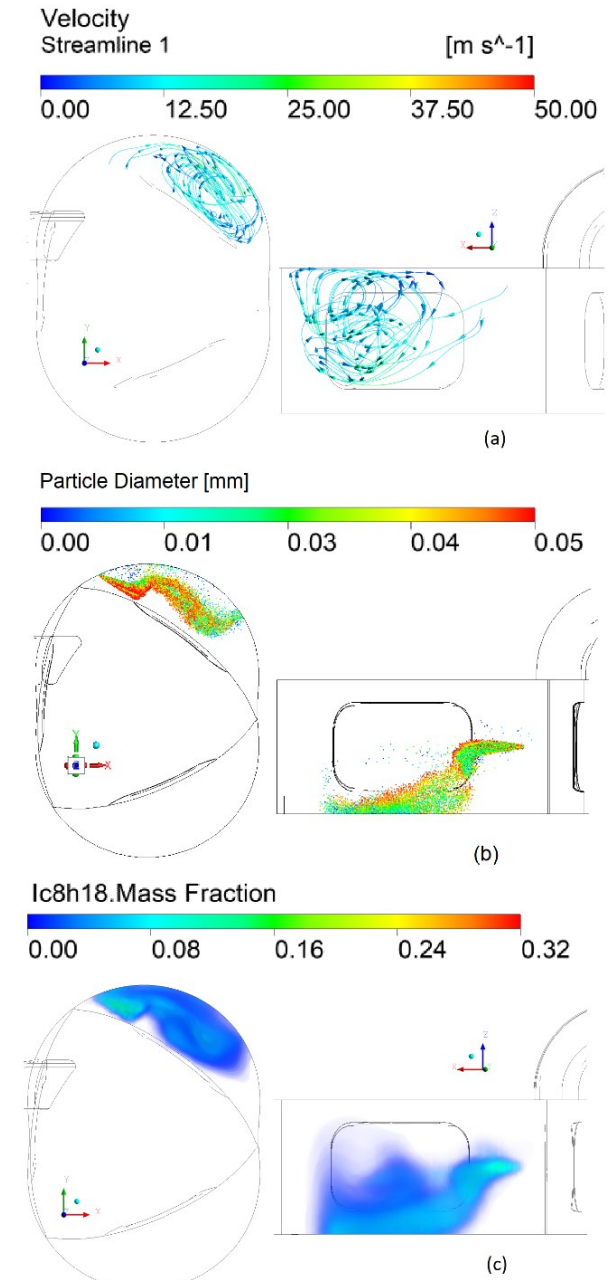


Figure 6. Mixture formation at the end of injection; (a) Flow velocity streamlines, (b) Droplet diameter and (c) Fuel mass fraction distributions at 110 ESA aBDC.

The flow streamlines become almost straight at 10 ESA bTDC as seen in Fig 7. Accumulated fuel vapor and few droplets driven to the leading side form rich mixture zone at leading side region. However, the distribution of fuel mass fraction in Fig. 7 shows that very lean mixture ($\lambda \sim 3$) is formed at the vicinity of spark plugs. There are also very few droplets left at the leading side of the rotor, which evaporates completely at 20 aTDC.

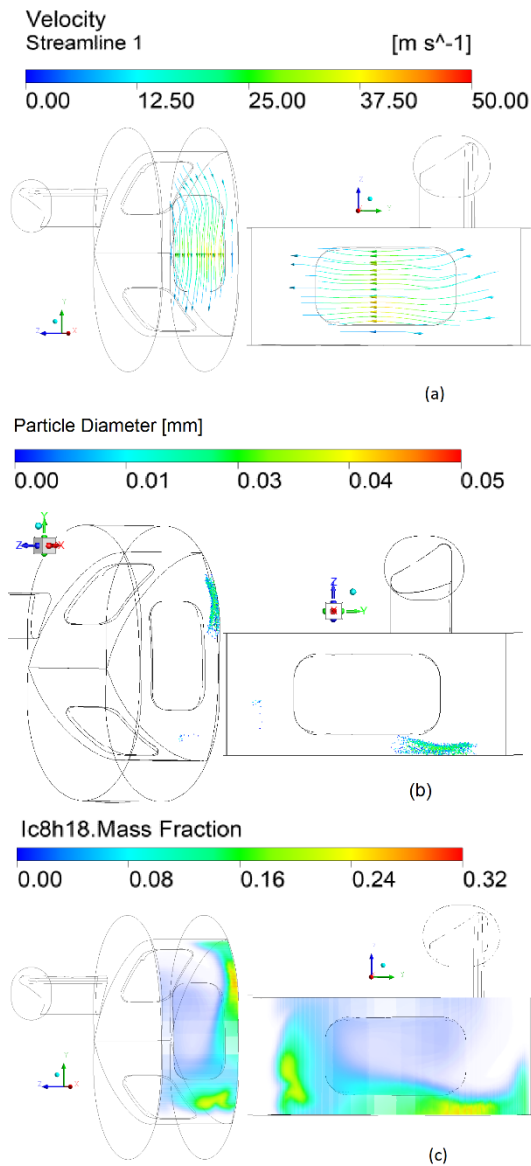


Figure 7. Mixture formation at the end of compression stroke; (a) Flow velocity streamlines, (b) Droplet diameter and (c) Fuel mass fraction distributions at 10 ESA bTDC.

5. Conclusions

In this study mixture formation in a side ported direct injection WTRE was numerically investigated. The below generalized conclusions are made for low pressure direct injection case that are utilized just after the inlet port closing.

1. After the injection, the spray droplets are driven by the swirl motion of the flow. The swirl motion is transformed to tumble motion due to decreasing volume of the chamber and rotor movement during in middle and last part of the compression stroke. However, the droplets are accumulated on the counter side of the inlet port.

2. Since the stratified location is not in the recess of the rotor, it is concluded that application of an early direct injection is not feasible for the existing engine geometry. Stable combustion is not anticipated at these conditions.

3. Flow velocity decreases during last part of the compression stroke. The tumble flow motion is centered close to the leading edge. It is concluded that an injection utilized at last part of the compression stroke is possible to get less effected from initial swirl motion and form more suitable stratification than an early injection.

Nomenclature

$C_{1\varepsilon}$	Constant term in RNG k- ε model
$C_{2\varepsilon}$	Constant term in RNG k- ε model
C_F	Constant term in TAB model
C_k	Constant term in TAB model
C_d	Constant term in TAB model
C_b	Constant term in TAB model
d	Damping constant
F	Force [N]
k	Spring constant
m	Mass [kg]
k	Turbulence kinetic energy [cm ² /s ²]
R_ε	Additional term in RNG k- ε model
S_k	Source term in RNG k- ε model
x	Displacement [m]
β	Constant term in RNG k- ε model
ε	Turbulence dissipation rate [cm ² /s ³]
λ	Stoichiometric ratio
ρ	Density [kg/m ³]
ρ_l	Droplet density [kg/m ³]
ρ_g	Gas density [kg/m ³]
μ	Viscosity [kg/m.s]
μ_{eff}	Effective viscosity [kg/m.s]
μ_l	Droplet viscosity [kg/m.s]

Acknowledgement

This work has been supported by TUBITAK (Turkish Scientific and Technical Research Council), Project no: 115M690.

6. References

- Okimoto, H., Ohzeki, H., & Kawachi, M., "Improvement of rotary engine performance by new induction system." SAE transactions, 387-397, (1983).
- Shimizu, R., Okimoto, H., Tashima, S., & Fuse, S., "The characteristics of fuel consumption and exhaust emissions of the side exhaust port rotary engine." SAE transactions:

- 821-828, (1995).
3. Ohkubo, M., Tashima, S., Shimizu, R., Fuse, S., & Ebino, H., "Developed technologies of the new rotary engine (RENESIS)." No. 2004-01-1790. SAE Technical Paper, (2004).
 4. Yamamoto, K., & Kuroda, T., "Toyo Kogyo's Research and Development on Major Rotary Engine Problems." SAE Transactions: 216-228, (1970).
 5. Yamamoto, K., Muroki, T., & Kobayakawa, T., "Combustion characteristics of rotary engines." SAE Transactions, 1296-1302, (1972).
 6. Eberle, M. K., & Klomp, E. D., "An evaluation of the potential performance gain from leakage reduction in rotary engines." SAE Transactions, 454-460, (1973).
 7. Nguyen, H. L., Addy, H. E., Bond, T. H., Lee, C. M., & Chun, K. S., "Performance and efficiency evaluation and heat release study of a direct-injection stratified-charge rotary engine." No. 870445. SAE Technical Paper, (1987).
 8. Jeng, D. Z., Hsieh, M. J., Lee, C. C., & Han, Y., "The numerical investigation on the performance of rotary engine with leakage, different fuels and recess sizes." No. 2013-32-9160. SAE Technical Paper, (2013).
 9. Picard, M., Tian, T., & Nishino, T., "Predicting Gas Leakage in the Rotary Engine—Part II: Side Seals and Summary." Journal of Engineering for Gas Turbines and Power 138, no. 6, 062504, (2016).
 10. Jones C., "A progress report on Curtiss-Wright's rotary stratified charge engine development." No. 741206. SAE Technical Paper, (1974).
 11. Jones, C., Lamping, H. D., Myers, D. M., & Loyd, R. W., "An Update of the Direct Injected Stratified Charge Rotary Combustion Engine Developments at Curtiss-Wright." No. 770044. SAE Technical Paper, (1977).
 12. Jones C., "An Update of Applicable Automotive Engine Rotary Stratified Charge Developments." No. 820347. SAE Technical Paper, (1982).
 13. Jones C., "Advanced Development of Rotary Stratified Charge 750 and 1500 HP Military Multi-Fuel Engines at Curtiss-Wright." No. 840460. SAE Technical Paper, (1984).
 14. Yamamoto, K., & Muroki, T., "Development on exhaust emissions and fuel economy of the rotary engine at Toyo Kogyo." No. 780417. SAE Technical Paper, (1978).
 15. Kagawa, R., Okazaki, S., Somyo, N., & Akagi, Y., "A study of a direct-injection stratified-charge rotary engine for motor vehicle application." SAE Transactions, 918-926, (1993).
 16. Hasegawa, Y., & Yamaguchi, K., "An experimental investigation on air-fuel mixture formation inside a low-pressure direct injection stratified charge rotary engine." No. 930678. SAE Technical Paper, (1993).
 17. Moriyoshi, Y., Muroki, T., & Xu, W., "A study on combustion characteristics of DISC rotary engine using a model combustion chamber." SAE transactions, 1653-1666, (1994).
 18. Muroki, T., Gotou, S., & Morita, K., "A Study of an Outline of Combustion for a Direct Injection Stratified-Charge Rotary Engine." No. 901600. SAE Technical Paper, (1990).
 19. Muroki, T., Moriyoshi, Y., & Takagi, M., "Combustion Characteristics of a Direct Injection Stratified Charge Rotary Engine Using Spark Ignition and Pilot Flame Ignition Systems." No. 2002-32-1791. SAE Technical Paper, (2002).
 20. Zhou, N. J., Pei, H. L., Gao, H. L., & Zhou, P., "Effects of Rotor Recess Geometries on Combustion Process in Diesel Rotary Engine." In ASME 2008 International Mechanical Engineering Congress and Exposition, pp. 255-259. ASME, (2008).
 21. Grasso, F., Wey, M. J., Bracco, F. V., & Abraham, J., "Three-dimensional computations of flows in a stratified-charge rotary engine." SAE transactions 9-75, (1987).
 22. Abraham, J., Wey, M. J., & Bracco, F. V., "Pressure non-uniformity and mixing characteristics in stratified-charge rotary engine combustion." SAE transactions, 1146-1159, (1988).
 23. Abraham J., and Bracco, F. V., "Fuel-air mixing and distribution in a direct-injection stratified-charge rotary engine." SAE Transactions, 515-526 (1989).
 24. Abraham J., and Bracco, F. V., "3-D Computations to improve combustion in a stratified-charge rotary engine - Part III: Improved ignition strategies." No. 920304. SAE Technical Paper, (1992).
 25. Jones C., "A New Source of Lightweight, Compact Multifuel Power for Vehicular, Light

Aircraft and Auxiliary Applications: The Joint Deere Score™ Engines." In ASME 1988 International Gas Turbine and Aeroengine Congress and Exposition, American Society of Mechanical Engineers, (1988).

26. Mount, R. E., & LaBouff, G. A., "Advanced stratified charge rotary engine design." No. 890324. SAE Technical Paper, (1989).

27. Louthan L., "Development of a Lightweight Heavy Fuel Rotary Engine." No. 930682. SAE Technical Paper, (1993).

28. Lu, Y., Pan, J., Fan, B., Otchere, P., Chen, W., & Cheng, B., "Research on the application of aviation kerosene in a direct injection rotary Engine-Part 1: Fundamental spray characteristics and optimized injection strategies" *Energy Conversion and Management*, 195, 519-532, (2019).

29. Boretti, A., Jiang, S., & Scalzo, J., "A novel wankel engine featuring jet ignition and port or direct injection for faster and more complete combustion especially designed for gaseous fuels." No. 2015-01-0007. SAE Technical Paper, (2015).

30. Fan, B., Pan, J., Yang, W., Chen, W., & Bani, S., "The influence of injection strategy on mixture formation and combustion process in a direct injection natural gas rotary engine." *Applied energy* 187 663-674, (2017).

31. Meyer, A. E., & Shoemaker, C. R., "High speed electronic fuel injection for direct injected rotary engine." No. 950452. SAE Technical Paper, (1995).

32. Reke, M., Grobosch, S., & Niegetiet, K. "The Piezoelectric Controlled Carburetor." No. 2011-32-0528. SAE Technical Paper, (2011).

33. Ozcanli, M., Bas, O., Akar, M. A., Yildizhan, S., & Serin, H. "Recent studies on hydrogen usage in Wankel SI engine." *International Journal of Hydrogen Energy*, 43.(38), 18037-18045, (2018).

34. Shi, C., Ji, C., Wang, S., Yang, J., Ma, Z., & Ge, Y., "Combined influence of hydrogen direct-injection pressure and nozzle diameter on lean combustion in a spark-ignited rotary engine", *Energy Conversion and Management*, 195, 1124-1137 (2019).

35. Javadzadehkalkhoran, M., "Experimental analysis of direct injection in Wankel engine", Master Thesis, Istanbul Technical University,

(2018).

36. Cihan, Ö., Javadzadehkalkhoran, M., Doğan, H.E., Demirci, A., and Kutlar, O.A, "Conversion of Two Rotor Wankel Rotary Engine to Single Rotor Experimental Engine and Preliminary Results.", *International Journal of Advances on Automotive and Technology*, 198-206, (2017).

37. Taskiran, O. O., Calik, A. T., & Kutlar, O. A., "Comparison of flow field and combustion in single and double side ported rotary engine." *Fuel* 254, 115651, (2019).

38. ANSYS FLUENT 12.0 User's Guide, http://www.afs.enea.it/project/neptunius/docs/fluent/html/ug/main_pre.htm, 12/04/2019.